Mater. Res. Soc. Symp. Proc. Vol. 1322 © 2011 Materials Research Society
DOI: 10.1557/opl.2011.1104

Fabrication of Subsurface Metallic Nanoparticles For Enhanced Carrier Generation in Silicon-based Photovoltaics

Nirag Kadakia[1], Mengbing Huang[1], and Hassaram Bakhru[1]

[1]Ion Beam Laboratory, State University of New York, 1400 Washington Avenue, Albany, NY 12222, U.S.A.

ABSTRACT

Due to the low absorption coefficient of silicon in the bulk of the solar spectrum, the majority of silicon-based photovoltaic cells are at least 300 micrometers thick, limiting their economic feasibility. To achieve cost parity with conventional sources of energy, silicon-based photovoltaics have begun to move towards thinner substrates, on the order of a few micrometers; such thinner cells necessitate the use of light-trapping methods to increase the optical path length. Much research has begun investigating the use of trapped electromagnetic waves, or surface plasmons, to increase light scattering and interband carrier transition rates in the surrounding material. In one scheme, plasmonic modes can be supported through polarization of metallic nanoparticles. Past research has focused on the deposition of silver nanoparticles on the surface, and has shown that light absorbance can be increased markedly for certain bandwidths. Here, the relevant mechanism is increased lateral light scattering, which tends to guide the light into directions that are then totally internally reflected. When such metallic nanoparticles are polarized by incoming radiation, in addition to increased light scattering, the electric field in the vicinity of the nanoparticle is highly magnified. Such high fields can increase the carrier transition rates, and therefore the absorbance, in the surrounding silicon by orders of magnitude. The enhancement however decreases rapidly with the radial distance and is virtually diminished by 10 nm from the nanoparticle surface. Deposition on the surface of the solar cell, therefore, cannot exploit this effect, being isolated from the silicon by the passivating layer. It has been suggested that instead, such particles might be embedded into the silicon itself. To that end, we have developed a method to create subsurface silver nanospheres, using a combination of ion implantation, thermal deposition, and subsequent thermal annealing. By tailoring the implantation parameters, we can localize the layer of nanospheres and even create various bands at various depths. Through Rutherford backscattering and secondary ion mass spectroscopy characterization, we have found that the Ag has indeed annealed into the desired location. To ensure that the Ag has agglomerated to nanoparticles, we have confirmed this with TEM images and selected area diffraction patterns that indicate that such nanoparticles are indeed bulk phase silver and have diameters of 20-35 nanometers. This method can help realize more efficient surface plasmon-enhanced Si-based photovoltaics.

INTRODUCTION

Recent work in thin silicon-based photovoltaics has emphasized increasing the intrinsically weak absorbance of silicon through a variety of methods; in doing so, the economic viability of silicon solar cells can be maintained and indeed further improved by moving toward thinner silicon device layers whose absorbance is on par with thicker wafer-based cells. This can be done either by increasing the optical path length or by enhancing the band-to-band carrier transition rate. The first method is typically done through backside reflectors and/or angular scattering mechanisms. Previous groups have shown improvements by using photonic crystals as Bragg reflectors, diffraction gratings, and chirped reflectors; in these cases, path length is increased both by multiple reflection and total internal reflection [1,2,3] In addition, others have begun investigating the distinctive properties of metal nanoparticles atop dielectric media [4,5]. Within certain bandwidths, metal spheres can exhibit enhanced scattering both in the forward direction toward the device and at angles within the critical angle for total internal reflection.

Alternatively, the carrier transition rate may be direction enhanced by applying a strong perturbation, for example via an electromagnetic field. It can be shown that, in the case of electromagnetic radiation incident upon a dielectric or metal sphere the carrier transition enhancement is directly proportional to the polarizability of the particle squared [6]. The polarizability, in the case of sphere of radius a and dielectric constant ε_p in a dielectric medium of constant ε_m, is given by [7]

$$\alpha = 4\pi a^3(\varepsilon_p - \varepsilon_p) / (\varepsilon_p + 2\varepsilon_m) \quad (1)$$

This equation exhibits a resonance when $\varepsilon_p = -2\varepsilon_m$, known as the surface plasmon resonance (SPR), due to the fact that the electromagnetic fields are quantized oscillations, similar to bulk plasmons, but are confined to the surface of the particle. Clearly only a *metal* nanoparticle, whose dielectric constant is negative below its plasma frequency, is required to satisfy this equation. In turn, a very strong electric field results from incident radiation whose wavelength is such that this condition is fulfilled.

The carrier transition rate is, however, also proportional to a geometrical scattering factor that is a function only of the particle shape. This factor has a maximum at the particle's surface, yet in the case of a sphere, has diminished by 90% within a distance of $\sqrt{5}\cdot a$ from the particle surface **[6]**. Any enhancement will only occur in the near vicinity of the particle surface; it is therefore recommended that to exploit this effect, the particle must be placed within the absorbing medium itself, not on the surface as is typically done for photovoltaic devices of this nature.

To that end, we have investigated a method to fabricate silver nanoparticles within the bulk of a silicon substrate. The fabrication utilizes a combination of ion implantation, thermal deposition, and furnace annealing, and we have characterized the particle crystallinity, size, and concentration through Rutherford backscattering spectroscopy (RBS), transmission electron microscopy (TEM), and secondary ion mass spectroscopy (SIMS). In addition, we can tailor the depth of the Ag nanoparticles by tuning only the ion implant energy, leaving the other processes parameters unchanged. Our work is a significant step in investigating the performance of plasmon-enhanced silicon solar cells.

EXPERIMENTAL DETAILS

Motivation for use of silver

It is well-known that metals exhibit negative dielectric constants (considering the real part only) in the range below their plasma frequency. The physical intuition behind this is that the frequency of the incoming photon is "slow" enough that the electrons in the metal can quickly respond to the incoming field and screen it, preventing transmission. Thus, since the real part of the dielectric function is negative, the refractive index must be imaginary ($Re(\varepsilon) = n^2 - k^2 = n^2$ for low absorption) and the Fresnel reflection is therefore 100%. The plasma frequency is thus a measure of how well a metal can respond to incoming radiation. Group 11 metals—Ag, Cu, Au—exhibit plasma frequencies in the UV range, ~ few eV, and so are good candidates for exciting SPR by light in the range of the solar spectrum, as the dielectric frequency will be negative in the visible and IR. We have chosen to investigate Ag as a) it is highly mobile in Si and so can be gettered into nanoparticle form, b) exhibits relatively absorption, and c) does not form silicides. Figure 1 shows the plots of $-2\varepsilon_{Si}$ and ε_{Ag} versus wavelength—where they cross, the resonance condition is satisfied, around 780 nm. This wavelength is well within the solar spectrum, so we may expect that the resonance condition will be for solar radiation.

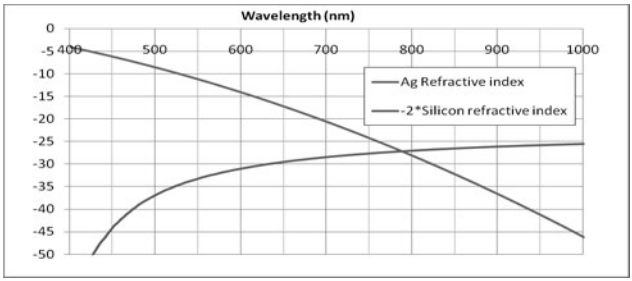

Figure 1. Plots of $-2\varepsilon_{Si}$ and ε_{Ag} as a function of wavelength. The intersection of the functions indicates where the denominator in eq. (1) vanishes, indicated a high polarizability.

Experimental setup

In our experiment, subsurface Ag nanoparticles were fabricated in CZ-grown silicon samples of ~300 μm thickness. The resistivity of the samples is in the range of 10-100 Ω-cm (p-Si), although the doping concentration is assumed immaterial for the processes considered here. Implantation was carried out using a Varian Extrion 400 keV ion implanter tool in an environment of pressure ~ 1e-6 torr. Thermal deposition was performed in a 1e-6 torr vacuum, and the furnace annealing was carried out in atmospheric pressure under a flowing nitrogen ambient at temperatures ranging from 600° C to 900° C. For RBS characterization, we used a 2 MeV Dynamitron implanter with a $^4He+$ species and XRUMP simulation software to determine the depth and concentration of the species. Bright field TEM characterization was performed on a JEOL 200CX microscope at magnifications from 60KX to 120KX, and selected area

diffraction patterns (SADP) were obtained using the same microscope. SIMS characterization was performed on an IonTof-V 300 time-of-flight SIMS system. The measurement beam was a 25keV pulsed Bi+ beam at 45 degrees incidence and the sputtering beam was 2keV Cs**,** also at 45 degrees incidence.

RESULTS

The RBS data of the samples implanted at various ion energies are shown in figures 2a, 2b, and 2c. The high energy edge of Ag is shown by the heavy black line, so the small peaks at channels 750, 675, and 550 in images a, b, and c, respectively, are those indicated by the Ag concentrations beneath the surface, corresponding to depths of 270, 550, and 1100 nm. The amount trapped Ag corresponds to a doses of about 5-7e15/cm^2. The corresponding SIMS data is

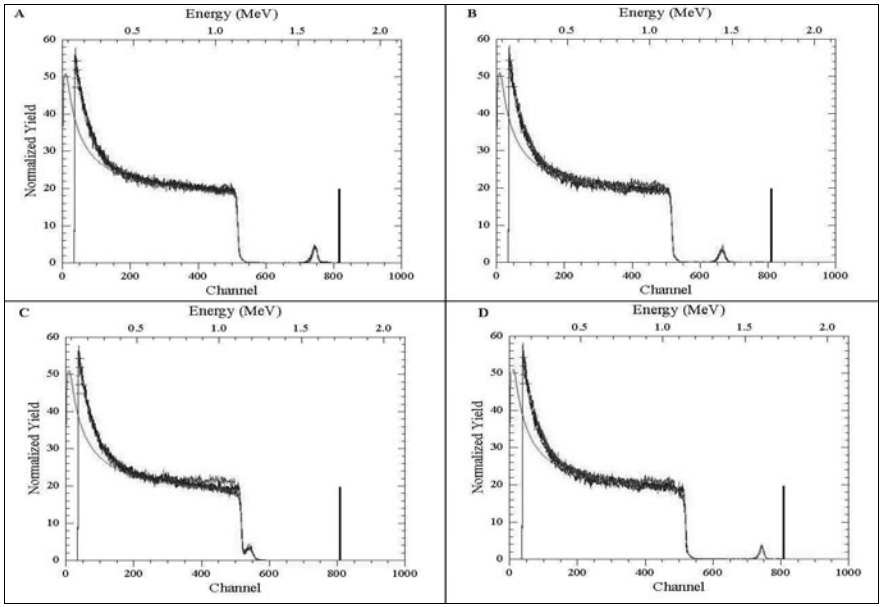

Figure 2. a), b), and c) RBS of samples corresponding to Ag depths of 270, 550, and 1100 nm. d) RBS data from of the sample in a), following further 900° C anneal

shown in figure 3, and indicates that the Ag is highly localized at the intended location. We have further annealed the samples at 900° C for 60 minutes, following the nanoparticle formation process. This is to simulate added heat treatments that a typical device would need to endure for the p-n junction formation, and to ensure that the nanoparticles do not disintegrate from their precipated form following the annealing. This data for the samples in figure 2a is shown in figure

2d, and it is clear that the total dose has diminished only slightly. To substantiate this data, we have also taken SIMS measurements; the sensitivity for our setup is two orders of magnitude lower than with RBS, and we find that the Ag is concentrated entirely at the depth intended, and there is no Ag (up to the SIMS background, about 3e17/cm^3) in the regions between the surface and the implant depth.

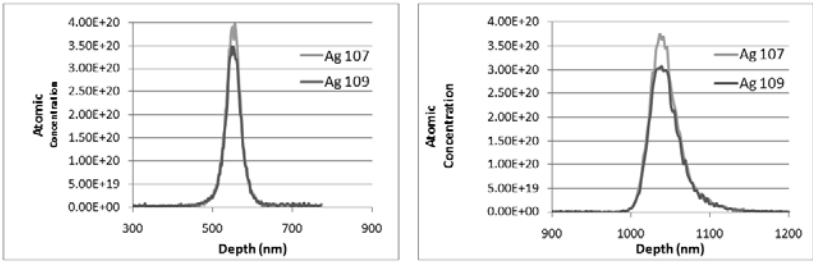

Figure 3. a) and b) SIMS data corresponding to the samples in figures 2b and 2c.

RBS characterization indicates that Ag has been trapped, but does not indicate the phase or bulk nature of the precipitates. For this we have taken TEM data, which is shown in figures 4a, 4b, and 4c. The bright field image shows the trapped Ag nanoparticles, evident through Z-contrast against the outerlying silicon. The diameters range from 20 – 35 nm. The crystallinity of these samples can be ascertained from the SADP images in figures 4b and 4c. Figure 4b shows the SADP along the <111> zone axis of the outerlying silicon, where the electron beam was not incident on the Ag band. A clear single crystal diffraction pattern of Si <111> can be seen. Figure 4c, on the other hand, shows the SADP of the area above the Ag band. Here, same <111> zone axis can be seen along with the <111> zone axis of Ag superimposed above it. The Ag is therefore precipitated in a bulk phase in the nanoparticles, rather than in atomic species, which would serve merely as recombination centers and would have no effect on the optical scattering or near field enhancement afforded by the SPR phenomenon.

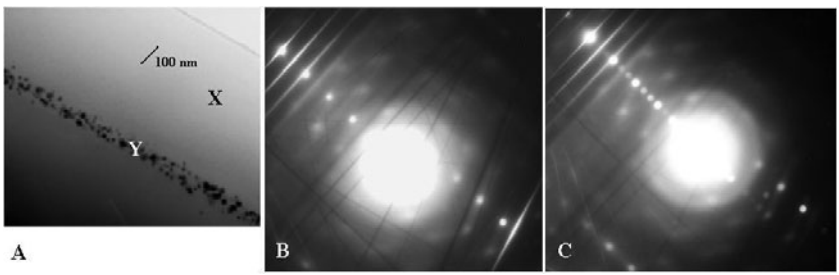

Figure 4. a) TEM bright field image of Ag nanoparticles. b) TEM SADP of region X in image 4a. c) TEM SADP of region Y in image 4a.

In conclusion, we have fabricated and characterized Ag nanoparticles within a crystalline silicon substrate using a combination of ion implantation, thermal deposition and furnace annealing. We have determined that their sizes are disperse, with diameters in the range of 20-35 nm, and that they form Ag in its bulk phase. Further work still needs to be done to test the impact of Ag on the bulk carrier lifetime, as it is generally accepted that transition metals in atomic form may have a highly detrimental effect on minority carrier lifetimes and recombination rates. This effect is not so important for thin Si solar cells, and if it can be shown that Ag precipitation does not reduce the carrier diffusion lengths significantly, the benefits of their optical properties may outweigh such impacts. In addition, work still needs to be done to test the photocurrent enhancement in various wavelength ranges and determine the optimal placing of the Ag nanoparticles.

ACKNOWLEDGMENTS

We would like to acknowledge Steve Novak of the College of Nanoscale Science and Engineering for providing the SIMS characterization.

REFERENCES

1. C. Heine and R. Morf, *Applied Optics*, **34**, 2476 (1995).
2. I. J. Kuzma-Filipek, F. Duerinckx, E. Van Kerschaver, K. Van Nieuwenhuysen, G. Beaucarne, and J. Poortmans, *J. Appl. Phys.* **104,** 073529 (2008).
3. L. Zeng,1, P. Bermel, Y. Yi, B. A. Alamariu, K. A. Broderick, J. Liu, C. Hong, X. Duan, J. Joannopoulos,, and L. C. Kimerling, *Appl. Phys. Lett.* **93,** 221105 (2008).
4. S. Pillai, K. R. Catchpole, T. Trupke, and M. A. Green, *J. Appl. Phys.* **101**, 093105 (2007).
5. D. M. Schaadt, B. Feng, and E. T. Yu, *J. Appl. Phys.* **86,** 063106 (2006).
6. A. Luque, A. Martí, M. J. Mendes, and I. Tobías, *J. Appl. Phys.* **104** 113118 (2008).
7. C.F. Bohren and D. R. Huffman, *Absorption and Scattering of Light by Small Particles*. (John Wiley and Sons, New York, 1983) pg. 139.